

Evidence Against Carbonization of the Thin-Film
Filters of the *Extreme Ultraviolet Variability
Experiment* onboard the *Solar Dynamics
Observatory*

Charles Tarrío¹ · Robert F. Berg¹ ·
Thomas B. Lucatorto¹ ·
Francis G. Eparvier² ·
Andrew R. Jones² · Brian Templeman² ·
Donald L. Woodraska² ·
Marie Dominique³

© Springer

Abstract In spite of strict limits on outgassing from organic materials, some spacecraft instruments making long-term measurements of solar extreme ultraviolet (EUV) radiation still suffer significant degradation. While such measures

✉ C. Tarrío
charles.tarrío@nist.gov
R.F. Berg
robert.berg@nist.gov
T.B. Lucatorto
thomas.lucatorto@nist.gov
F.G. Eparvier
frank.eparvier@lasp.colorado.edu
A.R. Jones
andrew.jones@lasp.colorado.edu
B. Templeman
brian.templeman@lasp.colorado.edu
D.L. Woodraska
don.woodraska@lasp.colorado.edu
M. Dominique
marie.dominique@oma.be

¹ Sensor Science Division, National Institute of Standards and Technology, Gaithersburg, MD, 20899, USA

² Laboratory for Atmospheric and Space Physics, University of Colorado, 3665 Discovery Drive, Boulder, CO, 80303, USA

³ Royal Observatory of Belgium, Ringlaan Avenue Circulaire 3, 1180 Brussels, Belgium

have reduced the rate of degradation, they have not completely eliminated it in some cases. For example, in five years, the aluminum filters used in the *Extreme Ultraviolet Variability Experiment* (EVE) instruments onboard the *Solar Dynamics Observatory* (SDO) suffered losses exceeding 40% at 30.4 nm. Comparing those losses with the negligible losses of nearby zirconium filters on the same instruments indicated that the problem was not due to carbonization on the Sun-facing side of the filter. To investigate whether the loss was due to carbon deposition on the downstream face of the Al filter, we exposed the backsides of Al and Zr filters to EUV in the presence of a volatile organic solvent in the laboratory and concluded that this could not be the cause. Given that the residual gas composition in the SDO spacecraft likely has water vapor as well as organics, these findings suggest that the transmission loss in the Al filter originated with oxidation caused by UV-activated adsorbed water.

Keywords: Instrumental Effects

1. Introduction

In the past several decades both the European Space Agency (ESA) and the National Aeronautics and Space Administration (NASA) have launched missions to observe the Sun at EUV wavelengths. Even though the emission at wavelengths below 100 nm accounts for less than 1% of the total solar radiation, it represents over 10% of the solar variability, and it provides a window on high energy events such as flares and coronal mass ejections (CMEs). Studying these events will improve our understanding of the solar dynamics which give rise to space weather, and leading to more timely forecasts of the CMEs that threaten many aspects of our modern technology.

Some of the optics in all these missions thus far have suffered serious degradation. This is the case for the *Solar Dynamics Observatory* (SDO), which was launched in 2010. Onboard was the Extreme Ultraviolet Variability Experiment (EVE), which included the *EUV spectrophotometer* (ESP) with five channels and two spectrometers (the Multiple EUV Grating Spectrometers MEGS-A and MEGS-B). A full description of the SDO Mission is given by Pesnell, Thompson, and Chamberlin (2012), and the EVE science objectives, instrument design, data products, and model developments are presented by Woods et al. (2012).

Contamination of optics in the presence of ionizing radiation is a well-known problem. As early as 1910, Berthelot and Gaudenchon (1910) observed deposition of carbon when a surface was illuminated with ultraviolet (UV) light in the presence of organic gases. The effect is well-known at synchrotron radiation laboratories, and it also causes degradation of filters used for order sorting and long-wavelength light blocking in long-term solar-monitoring spacecraft instruments.

Recent space-based instruments have often been equipped with duplicate filters to track degradation. On the SDO/EVE-MEGS-A spectrometer, the primary filter of each channel is periodically switched out for a reference filter within the same filter wheel. Those reference filters see little solar radiation:

only a few minutes per day for the secondary filter, or a few minutes per week for the tertiary. Comparing the transmissions of the primary filters with the reference filters gives an onboard estimate of the degradation of the primary filters. Comparison of spectral responsivity in overlapping passbands between the MEGS-A and ESP instruments is also used to give on-board evaluation of total instrument performance (the ESP instrument also has reference filters measured on the same cadence as those in MEGS-A). In addition to these onboard comparisons, recalibrations are performed every year or so with sounding rockets. A duplicate instrument is flown above the atmosphere on the rocket to make simultaneous observations along with the spacecraft instrument. Comparing the rocket and spacecraft measurements allows one to recalibrate the spacecraft instrument by using measurements that can be immediately tied back to the absolute, ground-based calibrations. These recalibrations sometimes reveal severe degradation, leading to large uncertainties in the previous period's spacecraft data. Instruments such as MEGS-A, ESP, and the *Solar EUV Monitor* (SEM) onboard the *Solar and Heliospheric Observatory* (SOHO) lost 50% to 80% of their original sensitivity at 30.4 nm (McMullin et al. (2002), BenMoussa et al. (2013)). The change in degradation trends between rocket underflights can also be due to operational changes in the instrument, for example bake-outs or other temperature events.

Driven by a concern over carbonization, personnel in mission design and preparation have been increasingly attentive to the choice of materials and maintenance of a high level of cleanliness in assembly and subsequent handling. Extreme care is used in selecting high radiation tolerance, ultra-high vacuum-compatible materials with low outgassing values and in keeping the use of any organic materials to a minimum. Spacecraft designs also now have better venting and improved thermal management to prevent the trapping of condensibles on critical optical components.

In spite of these efforts, progress in reducing the damage rate to instruments has been uneven. Two examples are the Al foil filters in two instruments onboard SDO, which was launched approximately 13 years after the SEM. The Al filters in both MEGS-A and the ESP showed losses of about 40% at the 30.4 nm line in the first year of service (BenMoussa et al., 2013) as shown in Figure 1.

We combined our analysis of the behaviors of the Zr and the Al filters in SDO with a set of laboratory experiments. The results rule out carbonization as the cause of the transmission loss.

2. SDO/EVE Observations and Results interpretation

Most UV/EUV-induced degradation of metallic filters in a variety of applications is due to either carbonization or oxidation. Previous degradation modeling for space optics has assumed carbon deposition to be the primary loss mechanism, likely because it is well known that under normal conditions many metals quickly form a stable, self-limiting oxide layer of a few nm thickness that is resistant to further oxidation. However, because of the similar absorption profiles of carbon (C) and oxygen (O) in the 7 nm to 35 nm region (see Figure 2), previous

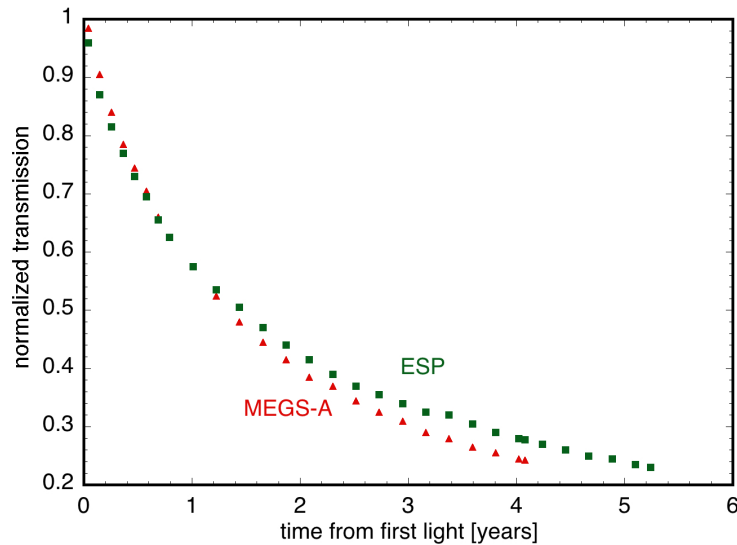


Figure 1. The Al filter transmission near 30 nm as a function of time in orbit for two instruments aboard the SDO mission. The MEGS-A and ESP are part of an instrument package called the *Extreme ultraviolet Variability Experiment*. The transmission loss in both instruments follows the same trend.

spectral absorption modeling (BenMoussa et al., 2013; McMullin et al., 2002) could not rule out oxidation as the loss mechanism. Given this ambiguity, we attempted to clarify the issue by first analyzing the existing data from the MEGS-A solar-observing instruments on SDO. While carbon growth is assumed to result from outgassing of organics, the oxidation is assumed to result from the photo-dissociation of water. We note that water vapor is the primary outgassing molecule for most vacuum systems, including spacecraft (Bieler et al., 2016).

Figure 3 shows the wavelength dependence of the degradation of the MEGS-A instrument. MEGS-A is a grazing incidence spectrograph covering the wavelength range of 6 nm to 37 nm with a resolution of approx 0.1 nm in two channels defined by the transmission of a Zr filter (MEGS-A1) and an Al filter (MEGS-A2). Figure 3 shows that the transmission of the Al channel dropped by 40% to 80% over its spectral range, while there was essentially no change in transmission across the Zr band. Most notably, in the overlap between the two channels, from 17 nm to 18 nm, there was virtually no decrease in the Zr channel but a 40% decrease in the Al channel. That decrease would correspond to about 40 nm of graphitic carbon growth.

Our analysis took three facts into account:

- i The absence of any significant transmission loss through the Zr filter ruled out significant carbon growth on either of its two faces.
- ii The Sun-facing sides of both the Al filter and the Zr filter experienced the same outgassing environment and radiation spectrum.

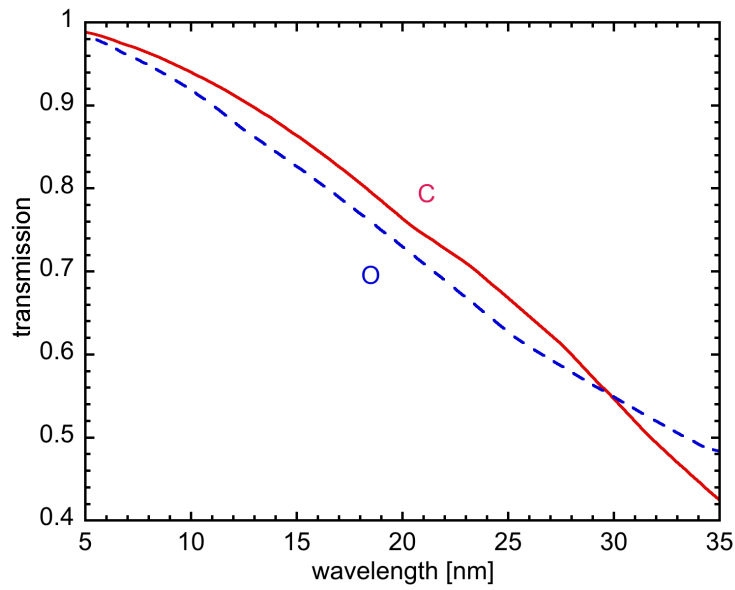


Figure 2. Calculated transmissions of 20 nm thicknesses of C and O. The transmission is calculated assuming a thin solid film 20 nm thick with a density of 2.0 g cm^{-3} for C and 1.0 g cm^{-3} for O with the optical constants taken from the CXRO database (Henke, Gullikson, and Davis, 1993).

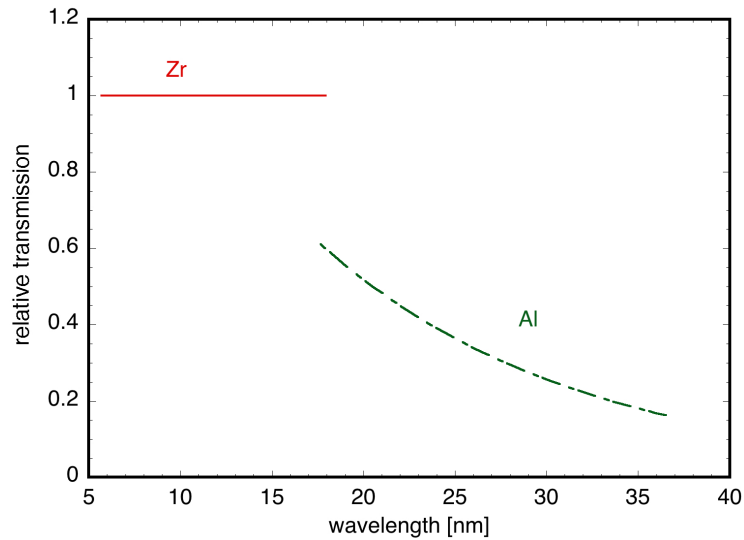


Figure 3. Wavelength dependence of the degradation seen by EVE-MEGS-A after four years of observation. The degradation in the Zr filter was negligible throughout its wavelength range. The striking contrast between the degradation in Al and in Zr in the wavelength overlap region near 18 nm is evidence that carbonization on the Sun-facing side of the filter was not the predominant cause of transmission loss.

- iii Experiments at the National Institute of Standards and Technology (NIST) (Hill et al., 2020) showed that while there is some substrate dependence in initial carbon growth rates, after one or two monolayers it is independent of the substrate.

Given these combined facts, we conclude that the lack of carbon growth on the Sun-facing side of the Zr filter clearly indicates that no carbon growth occurred on the Sun-facing surface of the Al filter either.

There is a second observation that supports the argument against carbonization: The temporal dependence of the degradation differs qualitatively from what one would expect from carbon growth. The left-hand panel of Figure 4 corresponds to the transmission data in Figure 1 using the attenuation length of 29 nm at wavelength 30.4 nm from the CXRO tables (Henke, Gullikson, and Davis, 1993). The corresponding carbon growth has a temporal dependence, and therefore a dose dependence that is approximately a square-root shape in time. In contrast, the carbon growth driven by outgassing with a plausible decay rate has no such temporal dependence. We considered the following decay rates, based in part on the outgassing behavior of vacuum systems (Grinham and Chew, 2017; O’Hanlon, 1980):

- i Diffusion of a contaminant out of a thick layer of material, such that $t \ll \tau$, where t is time, $\tau = L^2/(\pi^2 D)$ is a time constant, L is the layer thickness, and D is the diffusivity. The asymptotic decay rate goes as $t^{-1/2}$.
- ii Diffusion of a contaminant out of a thin layer of material. The asymptotic decay rate goes as $e^{-t/\tau}$.
- iii Desorption of a contaminant from surfaces. In vacuum systems at room temperature, this usually applies over days to water adsorbed on chamber walls made of stainless steel (Li and Dylla, 1995). The distribution of adsorption energies often gives a decay rate that goes approximately as t^{-1} .

In Figure 4, we combined each of those pressure decay rates with the recent model by Hill et al. (2020) that accurately accounts for the pressure-dependence of carbon growth. We approximated the growth rate predicted by that model as a function of pressure with a power law with an exponent about 0.1 in the region below 10^{-10} mbar. These all differ significantly from the square root dependence shown on the left-hand side of the figure. All of the resulting carbon growth rates shown in the right-hand panel of Figure 4 are nearly linear, and they differ significantly from the square-root dependence shown in the left-hand panel.

3. Experimental Setup and Results Interpretation

Thomas et al. (2010) and Tarrío et al. (2018) show that the UV-induced carbon growth rate has a strong wavelength dependence, with the growth rates at the longer wavelengths considerably higher. Given the longer wavelengths transmitted by Al relative to Zr, the carbon deposition rate on the instrument-facing

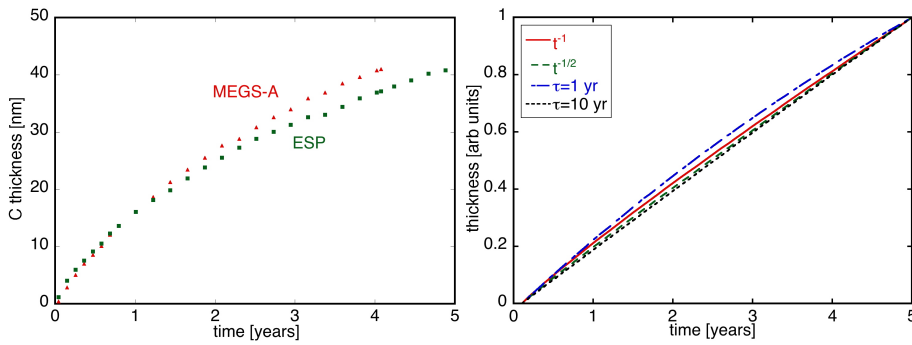


Figure 4. Left: thickness of deposited carbon calculated from the reduction in transmission of the filters at 30.4 nm in MEGS-A (red triangles) and ESP (green squares). Right: modeled carbon thickness assuming four different functional dependences of the contaminant pressure: t^{-1} (red solid); $t^{-1/2}$ (green dashed); and exponential decay with one year (blue chain) and ten year (black dotted) time constants.

surface of the Al filter could be higher, leading to the transmission losses. To see if this was a factor, we carried out experiments to investigate whether a difference of carbon deposition rates on the back faces of Al and Zr filters could explain the difference in the degradation of the two MEGS-A filters.

3.1. SURF Experimental Setup

To simulate prolonged exposure of the filters to solar radiation, we exposed the front sides of Al filters and Zr filters to broadband EUV/visible while maintaining a controlled pressure of organic vapor on the back side. We then determined the resulting carbon growth by measuring the difference in EUV transmission for each filter before and after exposure. These exposures took place at Beamline-1b of the NIST *Synchrotron Ultraviolet Radiation Facility* (SURF III) storage ring (Tarrío et al., 2011) as shown in Figure 5. Radiation from SURF III was reflected at 10 degree grazing angle of incidence from a Ru-coated toroidal mirror that collected and focused radiation with wavelengths longer than about 5 nm. The radiation passed through a thin-film filter captured in a gate valve before being focused to an elliptical spot 1 mm by 2.5 mm full-width at half maximum within a large chamber equipped with a leak valve that allowed controlled introduction of gases at low partial pressures. The filter normally serves as both a spectral filter and a vacuum seal that prevents the contaminant gas from flowing upstream to the mirror. Here, it was also the sample under investigation. The beam profile at the filter was constant in the horizontal dimension and a gaussian with roughly 3 mm FWHM in the vertical dimension. The base pressure is about 10^{-8} mbar and the maximum allowable partial pressure of introduced gas is about 10^{-3} mbar before upstreaming occurs.

On the downstream side of the filter, the emerging spectrum was the product of the irradiance from the source, the reflectance of the mirror, and the transmittance of the filter. Here the filters were either Al or Zr membranes similar to those flown on the SDO except for being thicker (250 nm vs. 150 nm) and backed

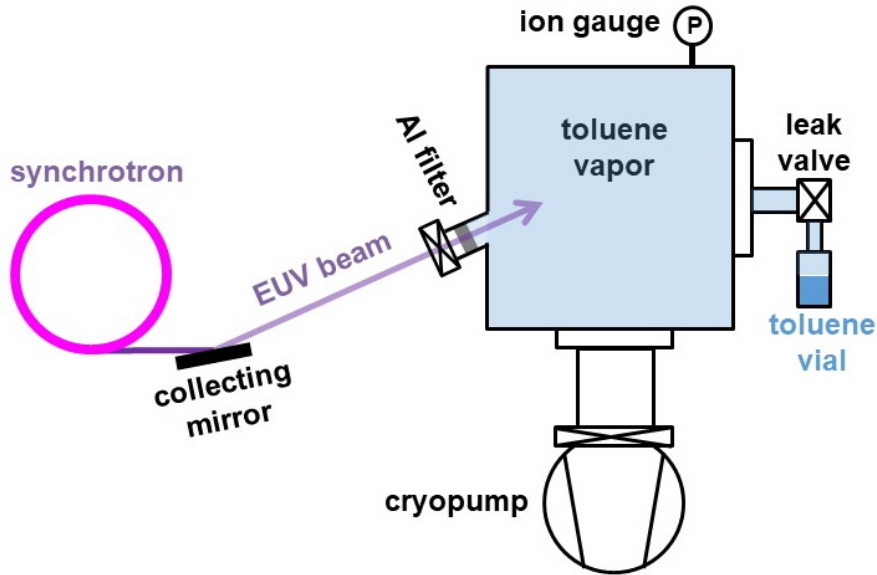


Figure 5. Radiation from SURF III was reflected from a Ru-coated toroidal mirror that collected and focused radiation with wavelengths longer than about 5 nm. The radiation passed through a thin-film filter captured in a gate valve before being focused within a large chamber equipped with a leak valve that allowed controlled introduction of toluene at low partial pressures.

with a copper mesh. The additional thickness and copper mesh were required for the filter to survive the high intensity of Beamline-1b (Tarrío et al., 2015).

Figure 6 shows the calculated spectra of radiation going through each filter. The spectra at the left are the product of the SURF irradiance, the mirror reflectance, and the filter transmittance. Those at the right are the product of the solar irradiance and the filter transmittance.

As mentioned, previous measurements indicated a strong wavelength dependence in the damage rates of mirror surfaces in the presence of organics. Thomas et al. (2010), using wide bandpasses, found that increasing the bandpass center from 14 nm to 60 nm increased the damage rate by about a factor of six, while NIST found that increasing the bandpass center from 13 nm to 65 nm caused an increase of about a factor of ten (Tarrío et al., 2018).

Because of the differences in the spectral distributions and thus the damage-causing potential from the two sources, simply equating the energy dose received from SURF with that received from the Sun was not suitable. We describe the effective dose leading to damage by introducing a weighting function to the dose:

$$\text{Dose}_{\text{eff}} = \tau \int I_{\text{source}}(\lambda) T_F(\lambda) W(\lambda) d\lambda \quad (1)$$

where τ is the time exposed; I is the irradiance from the source (either the Sun or the beamline); T_F is the transmission of the filter (either Zr or Al); W is

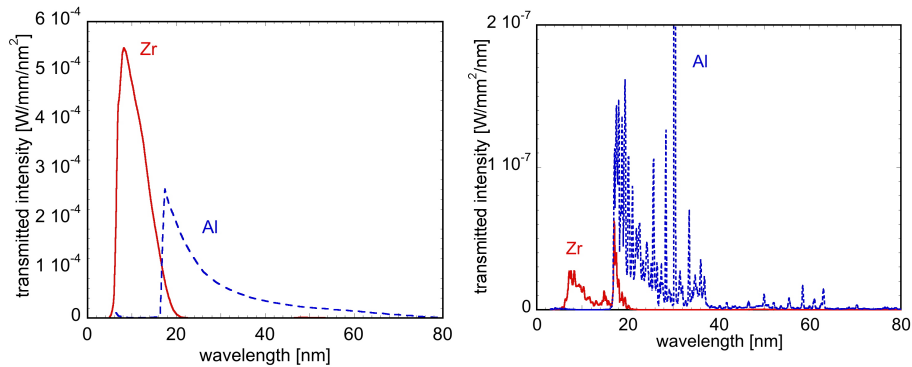


Figure 6. Left: the radiation from SURF Beamline-1b emerging from Zr and Al filters; Right: radiation from the Sun emerging through Zr and Al filters.

the weighting function; and λ is the wavelength. Boller et al. (1983) found that carbonization of synchrotron optics is primarily by secondary electrons, so we evaluated Equation 1 by assuming that $W(\lambda)$ is proportional to the secondary-electron yield. Henke, Knauer, and Premaratne (1981) developed a model for the secondary electron yield $Y_C(\lambda)$ from transmission photocathodes, which we have adapted for our case:

$$Y_C(\lambda) = K_C E \alpha_C(\lambda) \lambda_{eC} e^{(-\alpha_C t_C)} \tanh(t_C / 2\lambda_{eC}) \quad (2)$$

$$Y_m(\lambda) = K_m E \alpha_m(\lambda) \lambda_{em} e^{(-\alpha_m t_m)} \quad (3)$$

The subscripts C and m denote carbon or metal; K are material-dependent constants; E is the photon energy; α are the linear absorption coefficients; λ_e are the electron escape depths from the two materials; t are the material thicknesses. These differ slightly from those of Henke, Knauer, and Premaratne (1981). We assumed that the absorption coefficient is approximately equal to the ionization coefficient and that the metal thickness is much greater than the electron escape depth from the metal. As well, we have assumed that the carbon contamination is insulating (Dolgov et al., 2015).

For the absorption coefficients of the metal filters, we combined our own measurements between 7 nm and 34 nm with models based on data from the Center for X-ray Optics (CXRO) at Lawrence Berkeley National Laboratory (Henke, Gullikson, and Davis, 1993) to cover the range from 3 nm to 100 nm. For carbon we used only the CXRO data. Henke, Knauer, and Premaratne (1981) found electron escape depths of 4 nm for metals and up to 25 nm for insulators. We assumed 5 nm for our metallic filters, and we evaluated escape depths between 1 nm and 20 nm for carbon. We also estimated the yield for carbon thicknesses between 0 nm (bare metal) and 50 nm.

We evaluated the spectrally weighted electron yield $[Y(\lambda)]$ from 3 nm to 100 nm wavelength for both SURF and the Sun. We then integrated $Y(\lambda)$ to find the total electron yield per unit time for several electron-escape depths

and carbon thicknesses and calculated the total for three years' worth of solar exposure for each case. The required SURF exposure time was then evaluated for each case. The ratio of effective doses is only weakly dependent on the constants, including the escape depths, but the carbon thickness had a noticeable effect. We averaged every nanometer in thickness between 0 nm and 50 nm. The calculated exposure times were 60 minutes for Zr and 264 minutes for Al.

The exposed filters, although made by the same manufacturer¹ differed in three ways from those used on SDO: i) As mentioned previously, they were thicker and ii) backed by a copper mesh, while the spacecraft filters were backed by a nickel mesh or no mesh; iii) they had no oxidation-resistant coating, while on the spacecraft the Zr filter had a 20 nm C coat on both sides and the Al filter had a 20 nm C coat on the backside only. We expect that the coating had no effect on the carbon growth after the first two monolayers.

We chose toluene to be the representative contaminant because previous NIST contamination studies (Tarrío et al., 2018) showed it to have an intermediate carbonization rate among the several organic molecules tested. A vial of toluene was connected through a leak valve to the BL-1b sample chamber, to which the backside of the filter was exposed. The base pressure of this chamber was 10^{-8} mbar, and the admitted toluene pressure was 10^{-5} mbar as measured by an ionization gauge. The ionization-gauge sensitivity factor for toluene is 5.56 (Bartmess and Georgiadis, 1983), so the toluene partial pressure was likely lower than the ion-gauge reading by a factor of 0.2. Such an error is not significant since a factor of 100 in contaminant pressure leads to less than a factor of four increase in the carbon growth rate under EUV illumination (Hill et al., 2011).

The exposure times corresponded to three years of solar illumination, at which point the Al filters on the SDO spacecraft had losses of about 60% at 30.4 nm, corresponding to approximately 30 nm of carbon deposition. To ensure we were far from intensity saturation, where the amount of carbon deposition no longer depends linearly on dose, we carried out these experiments at reduced beam current (1 mA), which leads to intensities that are known to be well into the linear regime, and a few years solar exposure could be carried out in a reasonable amount of time. These were the conditions under which we exposed the Al filter for 264 minutes and the Zr filter for 60 minutes.

3.2. Experimental Results

Figure 6 shows the results of EUV transmittance measurements made before and after EUV exposure of the filters in the presence of toluene vapor. The Al and Zr filters were measured with radiation at 17.5 nm and 13.5 nm, respectively; both filters were nominally 250 nm thick. For both filters the transmittance increased by a fraction of a percent after the EUV exposure – this was likely due to photon-stimulated desorption of water or adventitious hydrocarbons and is commonly observed in spacecraft (Schläppi et al., 2010). In both cases there is clearly no

¹The filters were manufactured by Luxel Corporation. The identification of the manufacturer is for the purpose of providing information that may be relevant to the scientific purpose and is not to be construed as an endorsement of the product by NIST.

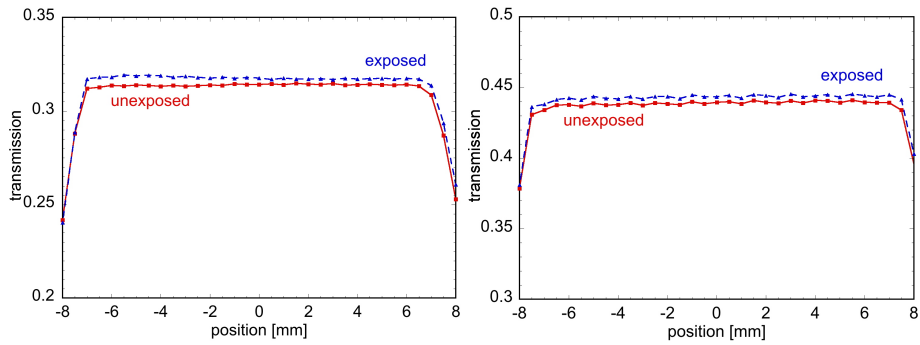


Figure 7. Left: Zirconium filter transmittances before (red) and after (blue) exposure to the equivalent of three-years' worth of solar radiation in the presence of toluene vapor. Right: the same for an aluminum filter. The slight increase was attributed to photon-stimulated desorption of water or adventitious hydrocarbons.

significant carbon growth. We also exposed filters to larger doses. Exposing a Zr filter to the equivalent of 50 years' solar dose grew only about 3 nm of carbon.

These results demonstrate that very little carbon could have grown on the instrument-facing, back side of the aluminum filters in SDO. The greatest uncertainty in our analysis lies in establishing the equivalence between the beam-line and solar doses. The transmission measurements have sub-percent uncertainty, (Tarrio et al., 2003) and even considering handling of the filters, can detect a 1% relative change in transmittance, which corresponds to about 0.5 nm of added carbon growth. As stated previously, the uncertainty in the partial pressure of toluene leads to a very small uncertainty in carbon growth. There is considerable uncertainty, however, in converting the solar and SURF spectra into damage-causing equivalents. Different models based on experimental results led to equivalences that differed by of order 20%. If we assume that the SURF dose is half what we estimated relative to the solar dose (1.5 years versus 3 years) in a worst case scenario, the anticipated carbon growth would have been 20 nm based on the transmission loss on the SDO, or 40 times the limits of our measurement.

4. Discussion and Lessons Learned

Sun-viewing spacecraft are now designed and constructed with careful attention toward minimizing the UV-induced growth of carbon on optics. Despite that attention, the Al filters on board SDO suffered significant degradation following its launch in 2010. In their review, BenMoussa et al. (2013) reasonably noted that the spectrum of that degradation was consistent with carbon growth on the filters. However, they were unable to explain the lack of degradation of a similar Zr filter. That puzzle can be explained if the degradation was caused by oxidation instead of carbonization. Oxidation is conceivable because carbon and oxygen have a similar absorption spectrum in the region from 5 nm to 35 nm.

Carbon growth certainly caused degradation in older Sun-viewing instruments, and we know of no previous study that considered oxidation as the cause

of an aluminum sun-viewing filter. Making the case for oxidation requires i) showing that carbonization is an insufficient explanation, and ii) showing that oxidation is a sufficient one. This paper addresses the first part by:

- i Noting the discrepancy between the Al and Zr filters in the MEGS-A instrument.
- ii Showing that the time dependence of the degradation is inconsistent with the time dependence of outgassing.
- iii Measuring negligible carbon growth on the back side of filters exposed to EUV and toluene vapor.

The insufficiency of carbonization as an explanation suggests but does not prove that the degradation was caused by oxidation. We are presently measuring and modeling the UV-induced oxidation of aluminum, and we plan to present those results in a later article. Here, we emphasize only that using clean materials and techniques to construct a Sun-viewing instrument may be insufficient to protect an aluminum filter.

5. Conclusions

The degradation of wavelength filters on solar-observing spacecraft instruments had been attributed to carbon growth for decades. Despite considerable effort to reduce organic outgassing, similar degradation has continued on newer spacecraft instruments with Al filters. Our examination of data from the SDO spacecraft found that a Zr filter experienced no transmission loss during five years, while a nearby Al filter degraded by 40 % at the same wavelength during the same interval, which would correspond to about 40 nm of carbon deposition. The difference between the two filters, which experience the same vacuum conditions, leads to the conclusion that carbon deposition on the sun-facing sides of the filters is not the cause of the degradation. We then studied the possibility of carbon growth on the backsides of multiple filters by using the NIST synchrotron to simulate three years of solar exposure while maintaining a low pressure of toluene vapor on the backside. Neither Al nor Zr suffered significant degradation, eliminating the possibility that carbon deposition on the backsides of the Al filters led to the reduced transmission on this mission. Degradation of Al filters caused by oxidation of the front surface remains a possibility. We are currently carrying out oxide-growth experiments at SURF III similar to the carbon-growth experiments described in this article. We expose aluminum filters to UV in an atmosphere of water vapor rather than toluene, and subsequently analyzed using EUV transmittance. Preliminary measurements indicate significant oxide growth, but further experiments are necessary to determine if oxidation is indeed responsible for all of the degradation.

6. Acknowledgments

This work was funded by NASA contract NNG07HW00C. We thank Shannon Hill, Dale Newbury, and Lee Richter for many helpful discussions.

7. Conflicts of Interest

The authors declare no conflicts of interest

References

- Bartmess, J.E., Georgiadis, R.M.: 1983, Empirical methods for determination of ionization gauge relative sensitivities for different gases. *Vacuum* **33**, 149 . [DOI](#).
- BenMoussa, A., Gissot, S., Schühle, U., Del Zanna, G., Auchère, F., Mekaoui, S., Jones, A.R., Walton, D., Eyles, C.J., Thuillier, G., Seaton, D., Dammasch, I.E., Cessateur, G., Mef-tah, M., Andretta, V., Berghmans, D., Bewsher, D., Bolsée, D., Bradley, L., Brown, D.S., Chamberlin, P.C., Dewitte, S., Didkovsky, L.V., Dominique, M., Eparvier, F.G., Foujols, T., Gillotay, D., Giordanengo, B., Halain, J.P., Hock, R.A., Irbah, A., Jeppesen, C., Judge, D.L., Kretzschmar, M., McMullin, D.R., Nicula, B., Schmutz, W., Ucker, G., Wieman, S., Woodraska, D., Woods, T.N.: 2013, On-orbit degradation of solar instruments. *Solar Phys.* **288**, 389. [DOI](#). [ADS](#).
- Berthelot, D., Gaudenchon, H.: 1910, The chemical effects of ultraviolet rays on gaseous bodies – the effects of polymerisation. *Comptes Rendus* **150**, 1169.
- Bieler, A., Altwegg, K., Balsiger, H., Berthelier, J.-J., Calmonte, U., Combi, M., De Keyser, J., Fiethe, B., Fuselier, S.A., Gasc, S., Gombosi, T., Hansen, K.C., Hässig, M., Korth, A., Le Roy, L., Mall, U., Rème, H., Rubin, M., Sémon, T., Tenishev, V., Tzou, C.-Y., Waite, J.H., Wurz, P.: 2016, Mass spectrometric characterization of the rosetta spacecraft contamination. *Proc. SPIE* **9952**, 99520E. [DOI](#).
- Boller, K., Haelbich, R.P., Hogrefe, H., Jark, W., Kunz, C.: 1983, Investigation of carbon contamination of mirror surfaces exposed to synchrotron radiation. *Nucl. Instrum. Methods* **208**, 273. [DOI](#).
- Dolgov, A., Lopaev, D., Lee, C.J., Zoethout, E., Medvedev, V., Yakushev, O., Bijkerk, F.: 2015, Characterization of carbon contamination under ion and hot atom bombardment in a tin-plasma extreme ultraviolet light source. *Appl. Surf. Sci.* **353**, 708. [DOI](#).
- Grinham, R., Chew, A.: 2017, A review of outgassing and methods for its reduction. *Appl. Sci. Converg. Technol.* **26**, 95. [DOI](#).
- Henke, B.L., Gullikson, E.M., Davis, J.C.: 1993, X-Ray Interactions: Photoabsorption, Scattering, Transmission, and Reflection at $E = 50\text{-}30,000$ eV, $Z = 1\text{-}92$. *Atomic Data Nuclear Data Tables* **54**, 181. [DOI](#). [ADS](#).
- Henke, B.L., Knauer, J.P., Premaratne, K.: 1981, The characterization of x-ray photocathodes in the 0.1-10-keV photon energy region. *J. Appl. Phys.* **52**, 1509. [DOI](#).
- Hill, S.B., Faradzhev, N.S., Richter, L.J., Grantham, S., Tarrío, C., Lucatorto, T.B., Yulin, S., Schürmann, V. M. and Nesterenko, Feigl, T.: 2011, Optics contamination studies in support of high-throughput EUV lithography tools. *Proc. SPIE* **7969**, 79690M. [DOI](#).
- Hill, S.B., Tarrío, C., Berg, R.F., Lucatorto, T.B.: 2020, Extreme-ultraviolet-induced carbon growth at contaminant pressures between 10^{-10} mbar and 10^{-6} mbar: Experiment and model. *J. Vac. Sci. Technol. A* **38**, 063201. [DOI](#).
- Li, M., Dylla, H.F.: 1995, Modeling of water outgassing from metal surfaces (iii). *J. Vac. Sci. Technol. A* **13**, 1872. [DOI](#).
- McMullin, D.R., Judge, D.L., Hilchenbach, M., Ipavich, F., Bochsler, P., Wurz, P., Burgi, A., Thompson, W.T., Newmark, J.S.: 2002, In-flight Comparisons of Solar EUV Irradiance Measurements Provided by the CELIAS/SEM on SOHO. *ISSI Scientific Reports Series* **2**, 135. [ADS](#).
- O'Hanlon, J.F.: 1980, *A user's guide to vacuum technology*, Wiley Interscience, New York. ISBN 978-0-471-27052-2.

-
- Pesnell, W.D., Thompson, B.J., Chamberlin, P.C.: 2012, The solar dynamics observatory (sdo). *Solar Phys.* **275**, 3. [DOI](#). [ADS](#).
- Schläppi, B., Altwegg, K., Balsiger, H., HäsSIG, M., Jäckel, A., Wurz, P., Fiethe, B., Rubin, M., Fuselier, S.A., Berthelier, J.J., de Keyser, J., Rème, H., Mall, U.: 2010, Influence of spacecraft outgassing on the exploration of tenuous atmospheres with in situ mass spectrometry. *J. Geophys. Res. (Space Phys.)* **115**, A12313. [DOI](#). [ADS](#).
- Tarrío, C., Grantham, S., Squires, M.B., Vest, R.E., Lucatorto, T.B.: 2003, Towards high-accuracy reflectometry for euv lithography. *J. Res. Natl. Inst. Stand. Technol.* **108**, 267. [DOI](#).
- Tarrío, C., Grantham, S., Hill, S.B., Faradzhev, N.S., Richter, L.J., Knjurek, C.S., Lucatorto, T.B.: 2011, A synchrotron beamline for extreme ultraviolet photoresist testing. *Rev. Sci. Instrum.* **82**, 073102. [DOI](#).
- Tarrío, C., Berg, R.F., Lucatorto, T.B., Lairson, B., Lopez, H., Ayers, T.: 2015, Thermally stable thin-film filters for high-power extreme-ultraviolet applications. *Rev. Sci. Instrum.* **86**, 116103. [DOI](#).
- Tarrío, C., Hill, S.B., Berg, R.F., Bajt, S.: 2018, Optics Contamination. In: Bakshi, V. (ed.) *EUV Lithography*, SPIE Press, Bellingham, WA, 335. ISBN 9780819469649.
- Thomas, P., Yankulin, L., Khopar, Y., Garg, R., Mbanaso, C., Antohe, A., Fan, Y.-J., Denbeaux, G., Aouadi, S., Jindahl, V., Wuest, A.: 2010, Wavelength dependence of carbon contamination on mirrors with different capping layers. *Proc. SPIE* **7636**, 76361X. [DOI](#).
- Woods, T.N., Eparvier, F.G., Hock, R., Jones, A.R., Woodraska, D., Judge, D., Didkovsky, L., Lean, J., Mariska, J., Warren, H., McMullin, D., Chamberlin, P., Berthiaume, G., Bailey, S., Fuller-Rowell, T., Sojka, J., Tobiska, W.K., Viereck, R.: 2012, Extreme ultraviolet variability experiment (eve) on the solar dynamics observatory (sdo): Overview of science objectives, instrument design, data products, and model developments. *Solar Phys.* **275**, 115. [DOI](#). [ADS](#).